Cell Reports
Medicine

Report

Long-term persistence of RBD$^+$ memory B cells encoding neutralizing antibodies in SARS-CoV-2 infection

Graphical abstract

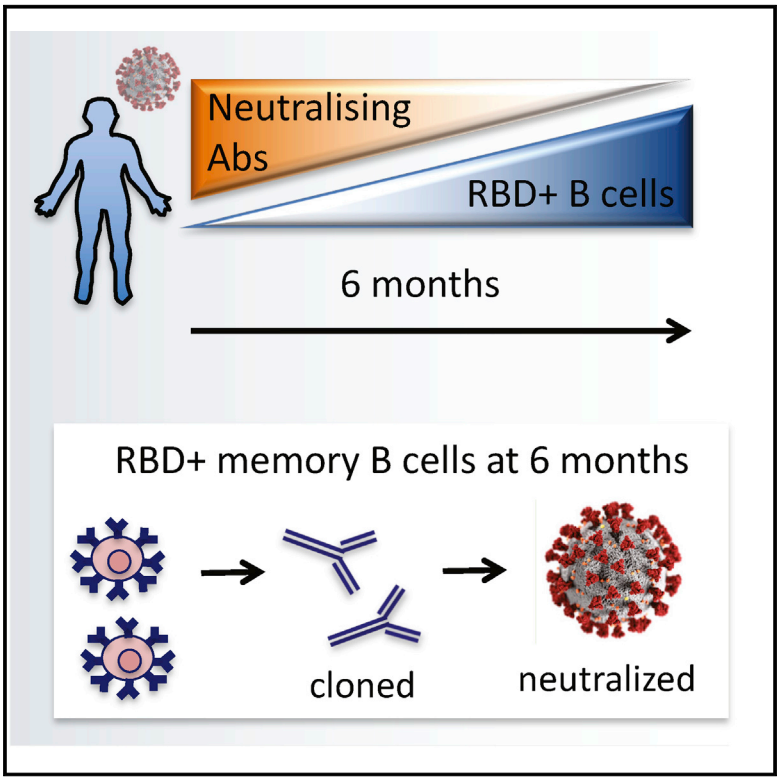

Highlights

- Decay of antibody binding to RBD and spike antigen after 6 months
- 11 of 81 (13.6%) participants revert to background neutralizing levels
- Despite declining antibody titers, robust memory B cell populations are observed
- Memory B cells retain potent neutralizing capacity

Authors

Arunasingam Abayasingam, Harikrishnan Balachandran, David Agapiou, ..., Marianne Martinello, Rowena A. Bull, on Behalf of the COSIN Study Group

Correspondence

r.bull@unsw.edu.au

In brief

Abayasingam et al. report that despite the declining anti-RBD antibody titers and neutralizing capacity of antibodies in the serum at 6 months, the memory B cells still contain RBD-specific reactivity that have the capacity to generate antibodies that can neutralize SARS-CoV-2 *in vitro*.

Abayasingam et al., 2021, Cell Reports Medicine 2, 100228
April 20, 2021
https://doi.org/10.1016/j.xcrm.2021.100228

CellPress

Cell Reports Medicine

CellPress
OPEN ACCESS

Report

Long-term persistence of RBD$^+$ memory B cells encoding neutralizing antibodies in SARS-CoV-2 infection

Arunasingam Abayasingam,[1,2,13] Harikrishnan Balachandran,[1,2,13] David Agapiou,[2] Mohamed Hammoud,[2] Chaturaka Rodrigo,[1,2] Elizabeth Keoshkerian,[2] Hui Li,[2] Nicholas A. Brasher,[1,2] Daniel Christ,[3] Romain Rouet,[3] Deborah Burnet,[3] Branka Grubor-Bauk,[4] William Rawlinson,[1,5] Stuart Turville,[2] Anupriya Aggarwal,[2] Alberto Ospina Stella,[2] Christina Fichter,[2] Fabienne Brilot,[6,7] Michael Mina,[8] Jeffrey J. Post,[9] Bernard Hudson,[10] Nicky Gilroy,[11] Dominic Dwyer,[11] Sarah C. Sasson,[2] Fiona Tea,[6,7] Deepti Pilli,[6,7] Anthony Kelleher,[2] Nicodemus Tedla,[1] Andrew R. Lloyd,[2] Marianne Martinello,[2,11,12,13] Rowena A. Bull,[1,2,13,14,*] and on Behalf of the COSIN Study Group

[1]School of Medical Sciences, Faculty of Medicine, UNSW Australia, Sydney, NSW, Australia
[2]The Kirby Institute, UNSW Australia, Sydney, NSW, Australia
[3]Garvan Institute of Medical Research, 384 Victoria Street, Darlinghurst 2010, NSW, Australia
[4]Virology Laboratory, Discipline of Surgery, The University of Adelaide and Basil Hetzel Institute for Translational Health Research, Adelaide 5011, SA, Australia
[5]Serology and Virology Division, Department of Microbiology, NSW Health Pathology, Prince of Wales Hospital, Sydney, NSW, Australia
[6]Faculty of Medicine and Health, School of Medical Sciences, The University of Sydney, Sydney, NSW, Australia
[7]Brain Autoimmunity Group, Kids Neurosciences Centre, Kids Research at the Children's Hospital at Westmead, Sydney, NSW, Australia
[8]Northern Beaches Hospital, Sydney, NSW, Australia
[9]Prince of Wales Clinical School, UNSW Australia, Sydney, NSW Australia
[10]Royal North Shore Hospital, Sydney, NSW, Australia
[11]Westmead Hospital, Sydney, NSW, Australia
[12]Blacktown Mt Druitt Hospital, Blacktown, NSW, Australia
[13]These authors contributed equally
[14]Lead contact
*Correspondence: r.bull@unsw.edu.au
https://doi.org/10.1016/j.xcrm.2021.100228

SUMMARY

Considerable concerns relating to the duration of protective immunity against severe acute respiratory syndrome-coronavirus-2 (SARS-CoV-2) exist, with evidence of antibody titers declining rapidly after infection and reports of reinfection. Here, we monitor the antibody responses against SARS-CoV-2 receptor-binding domain (RBD) for up to 6 months after infection. While antibody titers are maintained, ~13% of the cohort's neutralizing responses return to background. However, encouragingly, in a selected subset of 13 participants, 12 have detectable RBD-specific memory B cells and these generally are increasing out to 6 months. Furthermore, we are able to generate monoclonal antibodies with SARS-CoV-2 neutralizing capacity from these memory B cells. Overall, our study suggests that the loss of neutralizing antibodies in plasma may be countered by the maintenance of neutralizing capacity in the memory B cell repertoire.

INTRODUCTION

Virus and host immune factors affect the severity of acute infection and the subsequent quality and durability of immunological memory that will be established to protect against reinfection.[1] In severe acute respiratory syndrome-coronavirus-2 (SARS-CoV-2) infection, at least 80% of people infected appear to have asymptomatic or mild disease, while the remaining 20% are more severely unwell, with hyperactivation of the immune system leading to the excessive production of pro-inflammatory cytokines, lymphopenia, development of acute lung injury, and other end organ damage.[2–4] Age and disease severity have been linked with higher antibody titers and virus-specific neutralizing activity,[5] and it has been suggested that antibody responses may wane more quickly following mild illness,[6] although not all studies support these observations.[7,8]

As the coronavirus disease 2019 (COVID-19) pandemic continues to spread, the development of a prophylactic vaccine is critical.[9] A key component underpinning a successful vaccine design is an understanding of the characteristics of naturally occurring, potentially protective immunity. This includes both the immunological correlates of the initial control of viral replication, and the factors supporting establishment and long-term maintenance of adaptive immune responses. Evidence suggests that virus-specific B cell responses in people with SARS-CoV-2

Table 1. Characteristics of COSIN participants (n = 81)

		Infection severity		
	Total study population, n (%)	Asymptomatic or mild, n (%)	Moderate, n (%)	Severe, n (%)
Age, y, median (range)	52 (19–84)	54 (20–82)	47 (19–76)	72 (23–84)
Age, y, by category, n (%)				
<40	27 (33)	14 (29)	12 (41)	1 (25)
40 – 59	24 (30)	16 (33)	8 (28)	0 (0)
>60	30 (37)	18 (38)	9 (31)	3 (75)
Gender, n (%)				
Female	41 (51)	25 (52)	15 (52)	1 (25)
Male	40 (49)	23 (43)	14 (48)	3 (75)
Disease severity, n (%)				
Asymptomatic or mild	48 (59)	48 (100)	NA	NA
Moderate	29 (26)	NA	29 (100)	NA
Severe	4 (5)	NA	NA	4 (100)

COSIN, Collection of Coronavirus COVID-19 Outbreak Samples in New South Wales; NA, not applicable.

infection occur in conjunction with $CD4^+$ T follicular helper cell responses from ~1 week after symptom onset.[10–12] The first antibody responses target the N protein, whereas antibodies recognizing the S protein occur ~1 week later. Neutralizing antibody (NAb) responses, predominantly directed against the receptor-binding domain (RBD) of the S protein, develop within 2–3 weeks.[13] Most studies report very high rates of seroconversion to SARS-CoV-2,[5,14,15] followed by a rapid decline in RBD-specific antibody titers.[5,14,16] However, to date, most of these studies have only reported up to 4 months following infection. One recent study did report low titers of NAbs in one individual up to 7 months post-onset.[8]

In SARS-CoV-1 infection, the maintenance of durable NAb responses is unclear. Older studies suggest the initial specific IgG and NAb titers fall progressively over 2–3 years to become undetectable in up to 25% of individuals,[17] and a recent study demonstrated that low-titer SARS-CoV-1 NAbs were still detected in half of the group tested 17 years afterward.[18] Short-lived or low-titer NAb responses may not be a problem if robust memory B cell responses are generated and can be reactivated upon reinfection. However, memory B cell responses in SARS-CoV-1 may also be short-lived.[11] To date, only 2 studies have examined the SARS-CoV-2-specific memory B cell response beyond 4 months.[19,20] Encouragingly, both of these studies report that SARS-CoV-2-specific memory B cells are maintained, but no studies have yet reported whether these memory B cells present several months after infection can generate neutralizing antibodies upon reinfection.

In this study, we examined longitudinal antibody responses (anti-RBD, anti-Spike, and inhibitory capacity against a 50% infective dose [ID_{50}]) among 81 people with SARS-CoV-2 infection (confirmed by nucleic acid amplification testing [NAT]) at 2 time windows—1–3 and 4–6 months following symptom onset. We also assessed correlations between antibody titers in the blood and RBD-specific memory B cell frequency and the capacity of these memory B cells to make neutralizing antibodies.

RESULTS

Participants

Anti-RBD titers and neutralizing activity were analyzed in 81 participants at 2 follow-up time points (t1 and t2), calculated from the days post-onset of symptoms (DPS). Across all of the participants, t1 ranged from 30 to 87 DPS (median: 68, interquartile range [IQR]: 61–79 days) and t2 ranged from 110 to 181 DPS (median: 132, IQR: 118–151 days). The median time between sampling points (t2–t1) was 65 days (range: 31–126 days, IQR: 52–89 days). Participants had a median age of 51 years (IQR: 34–63.5 years) and 51% were female (n = 41) (Table 1). Most participants had mild (n = 47) or moderate (n = 29) COVID-19 illness, with 1 case of asymptomatic infection and 4 having severe disease.

RBD endpoint titer (EPT) and neutralizing activity

Assays to determine the EPT and neutralization activity were performed at 2 time points (t1 and t2) for all 81 participants. The RBD EPT was calculated from the dilution curve at the titration level equivalent to the optical density (OD) value equivalent to the mean + 2 standard deviations (SDs) from 19 healthy unexposed control participants. Neutralization activity was determined with a murine leukemia virus (MLV)-based SARS-CoV-2 Δ18 pseudovirus and a healthy control cutoff value of 22.61 (9.02 + 2 × 6.8), determined from the results of the same 19 healthy control participants.

At t1, 78 of 81 participants (96%) had RBD EPTs greater than the limit of detection (Figure 1A). In addition, 2 of the 3 non-reactive participants did not have antibodies against the Spike protein (Figure S1A). For neutralization activity with the pseudovirus assay, 54 of 81 participants (67%) had an ID_{50} above the cutoff (Figure 1B). At t2, the average ID_{50} and EPT values were significantly lower compared to t1 (mean difference [SEM] – ID_{50}: 37.3 (14.0), p = 0.009, EPT: 885 (258.4), p = 0.001), but 95% (77/81) and 74% (60/81) of participants had EPT and neutralization activity above the defined cutoffs (Figures S1B and S1C).

To validate the percentage of subjects that had undetectable levels of neutralization activity, ID_{50}s were also calculated with

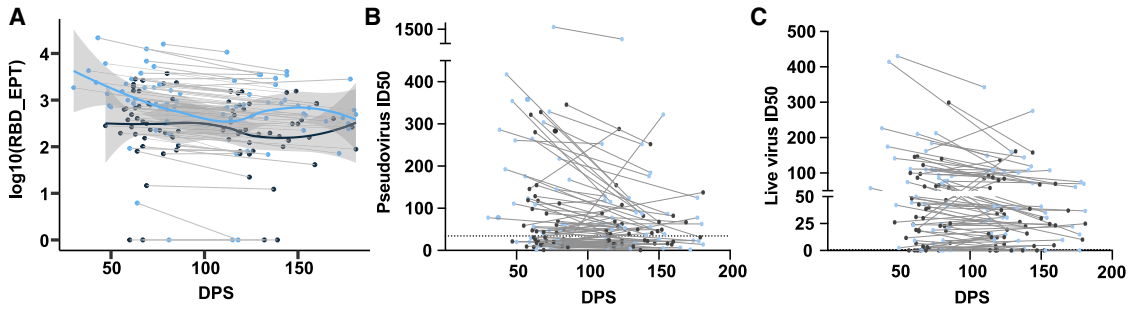

Figure 1. Antibody analysis

(A) RBD endpoint titers (EPTs) plotted against days post-onset of symptoms (DPS). Binding at each dilution was assessed in duplicate. The curve shows the mean EPT values using a Loess regression model. The shaded band indicates the 95% confidence interval. Blue datapoints highlight participants >51 years (median age) and black datapoints highlight participants <51 years.

(B) Neutralization half-maximal inhibitory serum dilution (ID_{50}) values determined with the pseudovirus assay plotted against the DPS. Infectivity at each dilution was assessed in triplicate and ID_{50} was determined using a normalized non-linear regression using GraphPad Prism software.

(C) ID_{50} values determined with the live virus assay plotted against DPS. Infectivity at each dilution was assessed in duplicate and ID_{50} was determined using a normalized non-linear regression using GraphPad Prism software. The lines connect a single subject sampled at 2 time points. The healthy control cutoff (mean + 2 × SD) is indicated by the dotted black line. Blue datapoints highlight participants >51 years (median age) and black datapoints highlight participants <51 years.

a live virus assay. The ID_{50} cutoff defined by the 19 healthy controls for the live virus was 0.6 (0.06 + 2 × 0.27). The live virus and pseudovirus data correlated (r = 0.65) (Figure S1G) and a similar trend in decline was observed between t1 and t2 (Figure 1C). At t1, 86.4% (70 of 81) of participants and at t2 86.4% (70 of 81) participants remained above the threshold for detectable neutralizing activity. Of these 11 participants at t1, 7 were below the threshold again at t2. For both neutralization assays, there were many participants who were only just above the threshold for neutralizing activity (Figures 1B and 1C). For all of the subsequent comparisons, the pseudovirus ID_{50} values were used.

EPT and pseudovirus ID_{50} values at t1 were strongly predictive of values at t2 (ID_{50} – r^2 = 0.862, $p < 0.001$, EPT – r^2 = 0.81, $p < 0.001$). EPT and ID_{50} results had a significant positive correlation at both time points (t1: r = 0.55, $p < 0.0001$, t2: r = 0.38, p = 0.0006) (Figures S1D and S1E). In unadjusted analysis, paired EPT values were associated with older age (p = 0.004) and the presence of diabetes mellitus, hypertension, or obesity (p = 0.011) when the sampling interval was included as a covariate. Gender, illness severity, immunosuppression, and history of smoking or current smoking, were not associated with paired EPT values (Table S1). In the adjusted analysis (metabolic comorbidity versus paired EPT measurements with sampling gap and age as covariates), the association with metabolic comorbidities disappeared, while that for age and EPT was borderline (p = 0.05) (Table S2). Paired ID_{50} values did not have a significant association with any of the demographic or clinical variables assessed in the unadjusted analysis (Table S3). There were also no significant associations between demographic and clinical variables and fold change in EPT or ID_{50} (t2 value/t1 value), except that a longer time between sample collections was associated with a greater fold decline of EPT and ID_{50} ($p < 0.05$).

RBD-specific memory B cells

The observed decline in neutralizing activity could be mitigated if a durable memory B cell response capable of generating neutralizing antibodies on demand is maintained. To assess the presence of a RBD-specific memory B cell response, 15 participants representing high (>1,000 EPT, n = 5), medium (EPT: 100–999, n = 7), and low EPT (EPT <100, n = 3) at t1 were selected, and their t1 and t2 peripheral blood mononuclear cells (PBMCs) were screened for RBD-specific $CD27^+$ memory B cells by flow cytometry. The 15 participants were generally representative of the broader study cohort, in relation to gender (female = 7), disease severity (mild = 4, moderate = 7, severe = 4), and age (range: 23–84). Six healthy uninfected participants were included as negative controls.

B cells were stained for flow cytometry, and the $CD19^+CD20^+CD10^-$ population was analyzed based on CD27, immunoglobulin D (IgD), IgG, and RBD binding phenotype (Figure S2A). Due to reports of lymphopenia in acute infection and concerns of skewed immune subsets, we compared the $CD27^+IgG^+RBD^+$ B cell frequency calculated both as per million PBMCs and per million B cells ($CD19^+CD20^+$) and found a strong correlation. Hence, all further analyses were calculated as per million B cells only (Figure S2B).

As the focus of this study was on the maintenance of virus-specific memory B cells, the analysis was performed on the $CD27^+RBD^+$ memory B cells and then sub-gated on the IgD and IgG phenotype (Figure 2A). The healthy participants had a high $CD27^+RBD^+IgD^+$ frequency (145.4 ± 95.4/10^6 B cells), but low $CD27^+RBD^+IgD^-IgG^+$ (15.7 ± 15.8/10^6 B cells) and $CD27^+RBD^+IgD^-IgG^-$ frequencies (20.3 ± 17.9/10^6 B cells) (Figure 2B). The Coronavirus Outbreak Samples in New South Wales (COSIN) participants generally had higher mean frequencies of all 3 virus-specific subsets than the healthy participants: $CD27^+RBD^+IgD^+$ (265.6 ± 314.2/10^6 B cells), $CD27^+RBD^+IgD^-IgG^+$ (251.3 ± 254.8/10^6 B cells), and $CD27^+RBD^+IgD^-IgG^-$ (52.3 ± 72.7/10^6 B cells) (Figure 2B). Despite some inter-subject variation, 12 of 15 participants had a $CD27^+RBD^+IgD^-IgG^+$ frequency above the healthy control derived cutoff at t2, and this was a significant increase from the same values observed at t1 (mean t1 = 165.8/10^6 B cells; mean t2 = 336.9/10^6 B cells; p = 0.0084) (Figure 2C). Two participants who did not have a $CD27^+RBD^+IgD^-IgG^+$ B cell

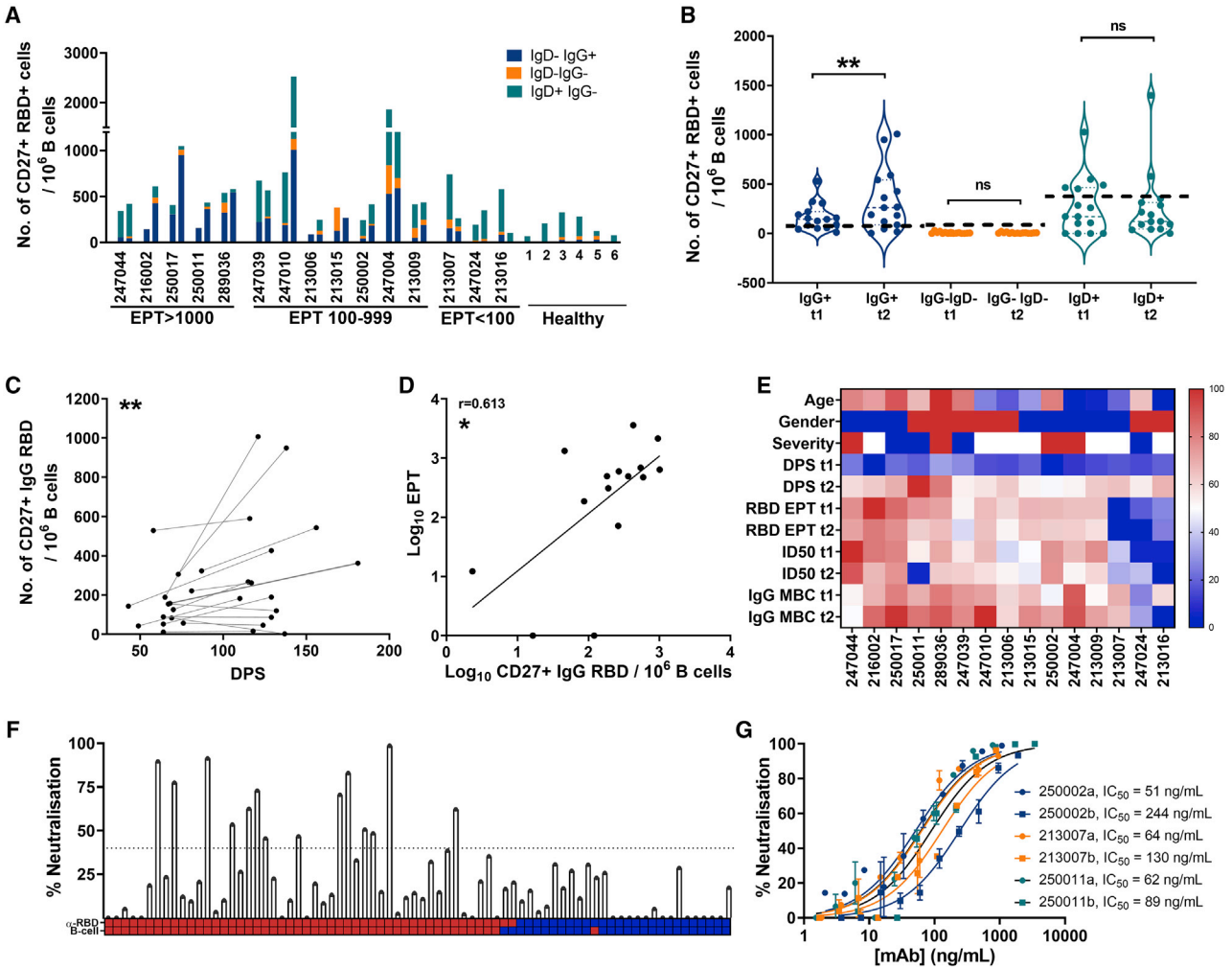

Figure 2. Memory B cell analysis and monoclonal antibody characteristics

(A) Distribution of RBD-specific Ig classes/10^6 B cells across all of the EPT groups. The first bar represents t1 and the second bar represents t2 of each SARS-CoV-2 participant. Healthy participants have 1 bar representing 1 time point.

(B) Violin plots of Ig subclass comparison between t1 and t2. Healthy control cut-off (mean + 2 × SD) are represented by the dotted black line.

(C) Comparison of $CD27^+IgG^+RBD^+$ B cells/10^6 B cells between t1 and t2 showing an increase in frequencies (Wilcoxon matched-pairs signed rank test, $p = 0.0084$).

(D) Correlation analysis between EPT and $CD27^+IgG^+RBD^+$ B cells/10^6 B cells during t2 (Spearman's correlation, $p = 0.017$).

(E) Heatmap of all subjects comparing age, gender, severity, DPS, EPT, ID_{50}, $CD27^+IgG^+RBD^+$ B cells/10^6 B cells from t1 and t2.

(F) Neutralization activity of all mAbs at 1/10 dilution. Dotted line represents 40% neutralization cutoff. Heatmap shows mAb RBD binding (red above and blue below cutoff) and the B cell line shows whether the originating memory B cell was IgG^+ (red) or IgD^+ (blue).

(G) Neutralization plot of 6 mAbs identified from 3 SARS-CoV-2 participants at t2. Each color represents a participant.

response greater than the healthy cutoff were from the low EPT group, and had mild or moderate clinical illnesses; the third was from the high EPT group, and this individual had severe disease. There was overall a strong correlation between IgG EPT and $CD27^+RBD^+IgD^-IgG^+$ B cell frequencies ($r = 0.613$, $p = 0.017$) at t2 (Figure 2D). No correlation between ID_{50}, gender, age, or disease severity and B cell frequencies was observed (Figures S2E–S2G).

RBD memory B cells with neutralizing capacity

To investigate whether these memory B cells were likely to have the capacity to induce NAb responses upon reinfection, the B cell receptor from single-cell sorted $CD27^+RBD^+$ cells from 5 participants were RT-PCR amplified and expressed as IgG1 monoclonal antibodies (mAbs) in Lenti-X 293T cells (Table 2). For this analysis, we selected 3 time points that had low to no detectable EPT and pseudovirus ID_{50} and 3 time points that had well above healthy cutoff titers. For participants who had a low IgG^+ cell frequency, IgD^+ cells were used (Table 2). A total of 76 mAbs were successfully synthesized as IgG from 49 IgG^+ cells and 27 IgD^+ cells, as determined by an anti-IgG ELISA. Of the 49 mAbs made from IgG^+ cells, 48 bound to RBD. From the IgD^+ B cells, 2 of the mAbs bound weakly to RBD. Antibody

Table 2. Monoclonal antibodies and their reactivity to RBD by subject

	Plasma characteristics		mAb characterstics				Neutralizing mAbs	
Subject ID	DPS	RBD titer	IgG derived	IgD derived	RBD binding	Neutralizing	IGHV usage	SHM (%)
61250-011	68	1,857.63	4	0	4	1		
	181	491.67	20	0	20	5	3–33, 1–58	6, 7
61213-007	132	0	15	0	15	6	4–31, 1–2	2, 5
61250-002	110	493.95	9	0	9	2	3–66, 4–39	5, 7
61213-016	137	12.24	1	12	2	0	–	–
61247-024	118	0	0	15	0	0	–	–

DPS, days post-onset of symptoms; IgD, immunoglobulin D; IgG, immunoglobulin G; mAb, monoclonal antibody; RBD, receptor-binding domain; SHM, somatic hypermutation.

containing supernatant was also diluted in 1 in 10 and screened for NAb activity with the SARS-CoV-2 pseudovirus. A neutralization percentage >40 was defined as having neutralizing activity. Of the 50 mAbs that bound RBD, 14 mAbs from 3 of the 5 participants had neutralizing activity (Table 2; Figure 2F). To further confirm the neutralizing activity, the IC_{50} was determined for the 2 highest NAbs from each of the 3 participants by quantifying the mAbs in the cell culture supernatant and performing neutralization assays on the SARS-CoV-2 pseudovirus (Figure 2G). No neutralizing antibodies were isolated from the 2 patients who did not seroconvert. Sequence analysis of these 6 potent mAbs revealed they were a mix of IGHV genes and had undergone affinity maturation, as indicated by a somatic hypermutation level of 2%–7%.

DISCUSSION

Recent data on SARS-CoV-2 anti-RBD and anti-Spike antibody responses have suggested a significant and rapid decline in titers after resolution of the clinical illness. Our observation is that despite declining EPT and ID_{50} values at 4–6 months following infection, most individuals retain binding and neutralization titers above background. Gender, disease severity, immunosuppression, comorbidities (diabetes mellitus, hypertension, obesity), and a history of smoking or current smoking, did not predict variation in ID_{50} or EPT over time.

A decline in antibody titers and neutralizing capacity following resolution of the clinical illness is not unusual, as seen in several other viral infections. However, the observation of antibody titers dipping below a detectable level is a concern for ongoing protection. Comparable declines in antibody titers would also be a significant concern following COVID-19 immunization.[20] Even though the vaccines against SARS-CoV-2 may not confer sterilizing immunity (as this is rarely observed in other vaccines approved for use), the capacity of such a vaccine to minimize disease, reduce viral shedding, and reduce transmission remains a highly desirable public health measure to control the pandemic.

The protective capacity of SARS-CoV-2 antibodies has recently been demonstrated in a candidate vaccine trial in rhesus macaques, in which 7 different vaccines were administered to 32 macaques. The development of NAbs was associated with protection against lung infection and nasal infection in all but 1 of the macaques.[21] In another study, passive immunization with a combination of NAbs in the monkeys correlated with the reduced development of pneumonia and lung damage.[22] These animal studies align with previous data on common coronaviruses, in which reinfections (and presumed ongoing NAb activity) were often associated with very mild or asymptomatic disease.[11] The very few validated cases of reinfection of SARS-CoV-2 have also been associated with mild or asymptomatic infection.[23]

Encouragingly our data show that despite the declining NAb titers, in the great majority of participants that seroconverted, memory B cells against RBD were maintained and even increased in numbers at 4–6 months following infection in 12 of 13 participants. This finding was similar to 3 other studies that also reported the maintenance and expansion of the RBD-specific IgG memory repertoire.[19,20,24] These 3 studies followed participants up to 5 months post-symptom onset. Our work extends beyond these studies in time, but also shows that the memory B cell population can generate potent NAbs. How long these memory B cells will continue to persist will be of significant interest. Tang et al.[25] reported that the memory B cell responses to SARS-CoV-1 were undetectable at 6 years. However, it is worth noting that Tang et al.[25] relied on ELISpot, with pooled vaccine-derived antigens to detect virus specific memory B cells, the standard assay at the time, whereas common methods now use purified antigen and flow cytometry, which are likely to be far more sensitive at detecting rare-frequency events.

Our study also identified a correlation between the frequency of RBD-specific memory B cells and RBD EPT, which indicates that RBD EPT may be a good and readily available marker for potential immunity. It is noteworthy, however, that the subject with the highest NAb titers had IgG RBD-specific memory B cells at the background level only. Interestingly, this participant had a severe illness, with prominent lymphopenia reported during the acute phase of infection. In addition, the loss of B cell germinal centers has been a feature reported in severe COVID-19 and could also account for the poor memory B cell response.[26] Further work should be conducted among people with severe COVID-19 to determine whether the apparent loss of circulating lymphocytes, which are recognized to include both T and B cells, and disruption to the B cell germinal centers negatively affects the frequencies or quality of the memory cell response.

In summary, most of the participants diagnosed with SARS-CoV-2 infection who initially had an RBD-specific

immune response had memory B cells persisting up to 6 months post-infection with the capacity to make neutralizing antibodies, despite falling NAb titers. The presence of memory B cells that produced NAbs following natural infection offers a clear hope of protective immunity sufficient to reduce reinfection severity upon re-exposure and a promise for effective vaccine strategies based on NAb induction and for herd immunity.

Limitations of study

The limited number of participants in this study did not allow for an expanded robust analysis of different comorbidities, age, or treatment on antibody and memory B cell dynamics; instead this study focused only on a subset grouped as metabolic disease.

The correlation of neutralization activity of participant sera between the live virus and pseudovirus assay was not as high as reported for some other studies, but technical differences between the assays may account for this. The assays used different cell lines (vero E6 and HEK293T-Ace2) and they were different lineages (D614G).

For determining the neutralization capacity of the memory B cell pool, antibodies were transiently expressed and screened, which does not provide an accurate measure of their potency due to differences in expression level. Only 6 antibodies had their IC_{50}s calculated, and therefore the proportion of memory B cells that encoded for neutralizing antibodies could actually be higher than the estimate here.

STAR★METHODS

Detailed methods are provided in the online version of this paper and include the following:

- KEY RESOURCES TABLE
- RESOURCE AVAILABILITY
  - Lead contact
  - Materials availability
  - Data and code availability
- EXPERIMENTAL MODEL AND SUBJECT DETAILS
  - Human subjects
  - Ethics statement
  - Cell lines
  - Primary cells
- METHOD DETAILS
  - RBD and spike protein production
  - RBD binding and limit of detection
  - Anti-Spike antibody assay
  - SARS-CoV-2 pseudovirus neutralisation assay
  - SARS-CoV-2 live virus neutralisation assay
  - Staining RBD memory B cells
  - Production of monoclonal antibodies from single-sorted RBD-specific B cells
- QUANTIFICATION AND STATISTICAL ANALYSIS

SUPPLEMENTAL INFORMATION

Supplemental information can be found online at https://doi.org/10.1016/j.xcrm.2021.100228.

ACKNOWLEDGMENTS

The authors would like to thank the study participants for their contribution to the research, as well as current and past researchers and staff. They would like to acknowledge members of the study group: protocol steering committee: Rowena A. Bull (co-chair, The Kirby Institute, UNSW Sydney, Sydney, Australia), Marianne Martinello (co-chair, The Kirby Institute), Andrew R. Lloyd (The Kirby Institute), John Kaldor (The Kirby Institute), Greg Dore (The Kirby Institute), Tania Sorrell (Marie Bashir Institute, University of Sydney, Sydney, Australia), William Rawlinson (New South Wales Health Pathology [NSWHP], NSW, Australia), Jeffrey J. Post (Prince of Wales Hospital [POWH]), Bernard Hudson (Royal North Shore Hospital [RNSH], Sydney, Australia), Dominic Dwyer (NSWHP), Adam Bartlett (Sydney Children's Hospital [SCH], Sydney, Australia), Sarah C. Sasson (UNSW), Nick Di Girolamo (UNSW), and Daniel Lemberg (SCH). Coordinating center: The Kirby Institute, UNSW Sydney, Sydney, Australia—Rowena A. Bull (coordinating principal investigator), Marianne Martinello (coordinating principal investigator), Marianne Byrne (clinical trials manager), Mohammed Hammoud (post-doctoral fellow and data manager), Andrew R. Lloyd (investigator), and Roshana Sultan (study coordinator). Site principal investigators: Jeffrey J. Post (POWH), Michael Mina (Northern Beaches Hospital [NBH], Sydney, Australia), Bernard Hudson (RNSH), Nicky Gilroy (Westmead Hospital, Sydney, Australia), William Rawlinson (NSWHP), Pam Konecny (St George Hospital [SGH], Sydney, Australia), Marianne Martinello (Blacktown Hospital, Blacktown, Australia), Adam Bartlett (SCH), and Gail Matthews (St Vincent's Hospital [SVH], Sydney, Australia). Site coordinators: Dmitrii Shek and Susan Holdaway (Blacktown Hospital), Katerina Mitsakos (RNSH), Dianne How-Chow and Renier Lagunday (POWH), Sharon Robinson (SGH), Lenae Terrill (NBH), Neela Joshi, (Lucy) Ying Li, Satinder Gill (Westmead Hospital), and Alison Sevehon (SVH). The Kirby Institute is funded by the Australian Government Department of Health and Ageing. The views expressed in this publication do not necessarily represent the position of the Australian Government. Research reported in this publication was supported by the Snow Medical Foundation as an investigator-initiated study. The content is solely the responsibility of the authors. R.A.B., M.M., C.R., and A.R.L. are fellows funded by the National Health and Medical Research Council (NHMRC). Some of the data presented in this work was acquired by instruments at the Mark Wainwright Analytical Centre (MWAC) of UNSW Sydney, which is in part funded by the Research Infrastructure Programme of UNSW.

AUTHOR CONTRIBUTIONS

Conceptualization, R.A.B., M.M., A.R.L., D.C., and N.T.; methodology, D.A., E.K., R.R., D.B., B.G.-B., S.T., and A.A.; investigation, A.A., H.B., D.A., N.A.B., F.T., D.P., A.O.S., C.F., and C.R.; writing – original draft, R.A.B., A.A., H.B., C.R., and D.A.; writing – review & editing, M.M., A.R.L., D.C., F.B., S.C.S., J.J.P., A.K., and D.D.; funding acquisition, R.A.B., M.M., and A.R.L.; resources, M.H., W.R., M.M., J.J.P., B.H., and N.G.; supervision, R.A.B., A.R.L., and M.M.

DECLARATION OF INTERESTS

The authors declare no competing interests.

INCLUSION AND DIVERSITY

We worked to ensure gender balance in the recruitment of human subjects. We worked to ensure that the study questionnaires were prepared in an inclusive way. One or more of the authors of this paper self-identifies as an underrepresented ethnic minority in science. One or more of the authors of this paper self-identifies as a member of the LGBTQ+ community. The author list of this paper includes contributors from the location where the research was conducted who participated in the data collection, design, analysis, and/or interpretation of the work.

Received: October 25, 2020
Revised: February 8, 2021
Accepted: March 9, 2021
Published: March 14, 2021

REFERENCES

1. Lucas, M., Karrer, U., Lucas, A., and Klenerman, P. (2001). Viral escape mechanisms–escapology taught by viruses. Int. J. Exp. Pathol. *82*, 269–286.
2. Huang, C., Wang, Y., Li, X., Ren, L., Zhao, J., Hu, Y., Zhang, L., Fan, G., Xu, J., Gu, X., et al. (2020). Clinical features of patients infected with 2019 novel coronavirus in Wuhan, China. Lancet *395*, 497–506.
3. Jiang, M., Guo, Y., Luo, Q., Huang, Z., Zhao, R., Liu, S., Le, A., Li, J., and Wan, L. (2020). T-cell subset counts in peripheral blood can be used as discriminatory biomarkers for diagnosis and severity prediction of Coronavirus disease 2019. J. Infect. Dis. *222*, 198–202.
4. Stringhini, S., Wisniak, A., Piumatti, G., Azman, A.S., Lauer, S.A., Baysson, H., De Ridder, D., Petrovic, D., Schrempft, S., Marcus, K., et al. (2020). Seroprevalence of anti-SARS-CoV-2 IgG antibodies in Geneva, Switzerland (SEROCoV-POP): a population-based study. Lancet *396*, 313–319.
5. Seow, J., Graham, C., Merrick, B., Acors, S., Pickering, S., Steel, K.J.A., Hemmings, O., O'Byrne, A., Kouphou, N., Galao, R.P., et al. (2020). Longitudinal evaluation and decline of antibody responses in SARS-CoV-2 infection. Nat. Microbiol. *5*, 1598–1607.
6. Long, Q.X., Liu, B.Z., Deng, H.J., Wu, G.C., Deng, K., Chen, Y.K., Liao, P., Qiu, J.F., Lin, Y., Cai, X.F., et al. (2020). Antibody responses to SARS-CoV-2 in patients with COVID-19. Nat. Med. *26*, 845–848.
7. Rydyznski Moderbacher, C., Ramirez, S.I., Dan, J.M., Grifoni, A., Hastie, K.M., Weiskopf, D., Belanger, S., Abbott, R.K., Kim, C., Choi, J., et al. (2020). Antigen-Specific Adaptive Immunity to SARS-CoV-2 in Acute COVID-19 and Associations with Age and Disease Severity. Cell *183*, 996–1012.e19.
8. Ripperger, T.J., Uhrlaub, J.L., Watanabe, M., Wong, R., Castaneda, Y., Pizzato, H.A., Thompson, M.R., Bradshaw, C., Weinkauf, C.C., Bime, C., et al. (2020). Orthogonal SARS-CoV-2 Serological Assays Enable Surveillance of Low-Prevalence Communities and Reveal Durable Humoral Immunity. Immunity *53*, 925–933.e4.
9. Funk, C.D., Laferrière, C., and Ardakani, A. (2020). A Snapshot of the Global Race for Vaccines Targeting SARS-CoV-2 and the COVID-19 Pandemic. Front. Pharmacol. *11*, 937.
10. Giménez, E., Albert, E., Torres, I., Remigia, M.J., Alcaraz, M.J., Galindo, M.J., Blasco, M.L., Solano, C., Forner, M.J., Redón, J., et al. (2021). SARS-CoV-2-reactive interferon-γ-producing CD8+ T cells in patients hospitalized with coronavirus disease 2019. J. Med. Virol. *93*, 375–382.
11. Vabret, N., Britton, G.J., Gruber, C., Hegde, S., Kim, J., Kuksin, M., Levantovsky, R., Malle, L., Moreira, A., Park, M.D., et al.; Sinai Immunology Review Project (2020). Immunology of COVID-19: current state of the science. Immunity *52*, 910–941.
12. Thevarajan, I., Nguyen, T.H.O., Koutsakos, M., Druce, J., Caly, L., van de Sandt, C.E., Jia, X., Nicholson, S., Catton, M., Cowie, B., et al. (2020). Breadth of concomitant immune responses prior to patient recovery: a case report of non-severe COVID-19. Nat. Med. *26*, 453–455.
13. Huang, A.T., Garcia-Carreras, B., Hitchings, M.D.T., Yang, B., Leah, C., Katzelnick, L.C., Rattigan, S.M., Brooke, A., Borgert, B.A., Moreno, C.A., Solomon, B.D., Trimmer-Smith, L., et al. (2020). A systematic review of antibody mediated immunity to coronaviruses: antibody kinetics, correlates of protection, and association of antibody responses with severity of disease. Nat. Commun. *11*, 4704.
14. Gudbjartsson, D.F., Helgason, A., Jonsson, H., Magnusson, O.T., Melsted, P., Norddahl, G.L., Saemundsdottir, J., Sigurdsson, A., Sulem, P., Agustsdottir, A.B., et al. (2020). Spread of SARS-CoV-2 in the Icelandic Population. N. Engl. J. Med. *382*, 2302–2315.
15. Ladhani, S.N., Jeffery-Smith, A., Patel, M., Janarthanan, R., Fok, J., Crawley-Boevey, E., Vusirikala, A., Fernandez Ruiz De Olano, E., Sanchez Perez, M., Tang, S., et al. (2020). High prevalence of SARS-CoV-2 antibodies in care homes affected by COVID-19; a prospective cohort study in England. EClinicalMedicine *28*, 100597.
16. Prevost, J., Gasser, R., Beaudoin-Bussières, G., Richard, J., Duerr, R., Laumaea, A., Anand, S.P., Goyette, G., Benlarbi, M., Ding, S., et al. (2020). Cross-sectional evaluation of humoral responses against SARS-CoV-2 Spike. Cell Rep. Med. *1*, 100126.
17. Cao, W.C., Liu, W., Zhang, P.H., Zhang, F., and Richardus, J.H. (2007). Disappearance of antibodies to SARS-associated coronavirus after recovery. N. Engl. J. Med. *357*, 1162–1163.
18. Tan, C.W., Chia, W.N., Qin, X., Liu, P., Chen, M.I., Tiu, C., Hu, Z., Chen, V.C., Young, B.E., Sia, W.R., et al. (2020). A SARS-CoV-2 surrogate virus neutralization test based on antibody-mediated blockage of ACE2-spike protein-protein interaction. Nat. Biotechnol. *38*, 1073–1078.
19. Vaisman-Mentesh, A., Dror, Y., Tur-Kaspa, R., Markovitch, D., Kournos, T., Dicker, D., Wine, Y., et al. (2020). SARS-CoV-2 specific memory B cells frequency in recovered patient remains stable while antibodies decay over time. medRxiv. https://doi.org/10.1101/2020.08.23.20179796.
20. Wheatley, A.K., Juno, J.A., Wang, J.J., Selva, K.J., Reynaldi, A., Tan, H.-X., Lee, W.S., Wragg, K.M., Kelly, H.G., Esterbauer, R., et al. (2020). Evolution of immunity to SARS-CoV-2. medRxiv. https://doi.org/10.1101/2020.09.09.20191205.
21. Mercado, N.B., Zahn, R., Wegmann, F., Loos, C., Chandrashekar, A., Yu, J., Liu, J., Peter, L., McMahan, K., Tostanoski, L.H., et al. (2020). Single-shot Ad26 vaccine protects against SARS-CoV-2 in rhesus macaques. Nature *586*, 583–588.
22. Baum, A., Ajithdoss, D., Copin, R., Zhou, A., Lanza, K., Negron, N., Ni, M., Wei, Y., Mohammadi, K., Musser, B., et al. (2020). REGN-COV2 antibody cocktail prevents and treats SARS-CoV-2 infection in rhesus macaques and hamsters. Science *370*, 1110–1115.
23. Gupta, V., Bhoyar, R.C., Jain, A., Srivastava, S., Upadhayay, R., Imran, M., Jolly, B., Divakar, M.K., Sharma, D., Sehgal, P., et al. (2020). Asymptomatic reinfection in two healthcare workers from India with genetically distinct SARS-CoV-2. Clin. Infect. Dis., ciaa1451.
24. Rodda, L.B., Netland, J., Shehata, L., Pruner, K.B., Morawski, P.A., Thouvenel, C.D., Takehara, K.K., Eggenberger, J., Hemann, E.A., Waterman, H.R., et al. (2020). Functional SARS-CoV-2-specific immune memory persists after mild COVID-19. Cell *184*, 169–183.e17.
25. Tang, F., Quan, Y., Xin, Z.T., Wrammert, J., Ma, M.J., Lv, H., Wang, T.B., Yang, H., Richardus, J.H., Liu, W., and Cao, W.C. (2011). Lack of peripheral memory B cell responses in recovered patients with severe acute respiratory syndrome: a six-year follow-up study. J. Immunol. *186*, 7264–7268.
26. Kaneko, N., Kuo, H.H., Boucau, J., Farmer, J.R., Allard-Chamard, H., Mahajan, V.S., Piechocka-Trocha, A., Lefteri, K., Osborn, M., Bals, J., et al.; Massachusetts Consortium on Pathogen Readiness Specimen Working Group (2020). Loss of Bcl-6-Expressing T Follicular Helper Cells and Germinal Centers in COVID-19. Cell *183*, 143–157.e13.
27. Tea, F., Lopez, J.A., Ramanathan, S., Merheb, V., Lee, F.X.Z., Zou, A., Pilli, D., Patrick, E., van der Walt, A., Monif, M., et al.; Australasian and New Zealand MOG Study Group (2019). Characterization of the human myelin oligodendrocyte glycoprotein antibody response in demyelination. Acta Neuropathol. Commun. *7*, 145.
28. Hoffmann, M., Kleine-Weber, H., and Pöhlmann, S. (2020). A Multibasic Cleavage Site in the Spike Protein of SARS-CoV-2 Is Essential for Infection of Human Lung Cells. Mol. Cell *78*, 779–784.e5.
29. Keck, Z.Y., Li, S.H., Xia, J., von Hahn, T., Balfe, P., McKeating, J.A., Witteveldt, J., Patel, A.H., Alter, H., Rice, C.M., and Foung, S.K. (2009). Mutations in hepatitis C virus E2 located outside the CD81 binding sites lead to escape from broadly neutralizing antibodies but compromise virus infectivity. J. Virol. *83*, 6149–6160.
30. Bartosch, B., Bukh, J., Meunier, J.C., Granier, C., Engle, R.E., Blackwelder, W.C., Emerson, S.U., Cosset, F.L., and Purcell, R.H. (2003). In vitro assay for neutralizing antibody to hepatitis C virus: evidence for broadly conserved neutralization epitopes. Proc. Natl. Acad. Sci. USA *100*, 14199–14204.

31. Kalemera, M.D., Capella-Pujol, J., Chumbe, A., Underwood, A., Bull, R.A., Schinkel, J., Sliepen, K., and Grove, J. (2021). Optimized cell systems for the investigation of hepatitis C virus E1E2 glycoproteins. J. Gen. Virol. *102*. https://doi.org/10.1101/2020.06.18.159442.

32. Crawford, K.H.D., Eguia, R., Dingens, A.S., Loes, A.N., Malone, K.D., Wolf, C.R., Chu, H.Y., Tortorici, M.A., Veesler, D., Murphy, M., et al. (2020). Protocol and Reagents for Pseudotyping Lentiviral Particles with SARS-CoV-2 Spike Protein for Neutralization Assays. Viruses *12*, E513.

33. Hoaglin, D.C. (1993). Revising a display of multidimensional laboratory measurements to improve accuracy of perception. Methods Inf. Med. *32*, 418–420.

34. Wu, B.R., Eltahla, A.A., Keoshkerian, E., Walker, M.R., Underwood, A., Brasher, N.A., Agapiou, D., Lloyd, A.R., and Bull, R.A. (2019). A method for detecting hepatitis C envelope specific memory B cells from multiple genotypes using cocktail E2 tetramers. J. Immunol. Methods *472*, 65–74.

35. Rizzetto, S., Koppstein, D.N.P., Samir, J., Singh, M., Reed, J.H., Cai, C.H., Lloyd, A.R., Eltahla, A.A., Goodnow, C.C., and Luciani, F. (2018). B-cell receptor reconstruction from single-cell RNA-seq with VDJPuzzle. Bioinformatics *34*, 2846–2847.

36. Liao, H.X., Levesque, M.C., Nagel, A., Dixon, A., Zhang, R., Walter, E., Parks, R., Whitesides, J., Marshall, D.J., Hwang, K.K., et al. (2009). High-throughput isolation of immunoglobulin genes from single human B cells and expression as monoclonal antibodies. J. Virol. Methods *158*, 171–179.

37. Gupta, N.T., Vander Heiden, J.A., Uduman, M., Gadala-Maria, D., Yaari, G., and Kleinstein, S.H. (2015). Change-O: a toolkit for analyzing large-scale B cell immunoglobulin repertoire sequencing data. Bioinformatics *31*, 3356–3358.

STAR★METHODS

KEY RESOURCES TABLE

REAGENT or RESOURCE	SOURCE	IDENTIFIER
Antibodies		
Streptavidin-PE	ThermoFisher Scientific	Cat#S21388
Streptavidin-APC	BD Biosciences	Cat#554067; RRID:AB_10050396
Fixable Viability Stain 700	BD Biosciences	Cat#564997; RRID:AB_2869637
Human Fc block	BD Biosciences	Cat#564220; RRID:AB_2869554
Stain brilliant buffer	BD Biosciences	Cat#566349; RRID:AB_2869750
B-ly4 (BV421) [Anti-CD21]	BD Biosciences	Cat#562966; RRID:AB_2737921
FA6-2 (BV510) [Anti-IgD]	BD Biosciences	Cat#563034; RRID:AB_2737966
HI10A (BV605) [Anti-CD10]	BD Biosciences	Cat#562978; RRID:AB_2737929
SJ25C1 (BV711) [Anti-CD19]	BD Biosciences	Cat#563036; RRID:AB_2737968
2H7 (APC-H7) [Anti-CD20]	BD Biosciences	Cat#560734; RRID:AB_1727449
G18-145 (BV786) [Anti-IgG]	BD Biosciences	Cat#564230; RRID:AB_2738684
N-T271 (PE-CF594) [Anti-CD27]	BD Biosciences	Cat#562297; RRID:AB_11154596
HIT2 (PE-Cy7) [Anti-CD38]	BD Biosciences	Cat#560677; RRID:AB_1727473
G46-6 (BB515) [Anti-HLA-DR]	BD Biosciences	Cat#564516; RRID:AB_2732846
SK7 (BB700) [Anti-CD3]	BD Biosciences	Cat#566575; RRID:AB_2860004
AffiniPure Goat Anti-Human IgG, F(ab')2 Fragment Specific	Jackson ImmunoResearch	Cat#109-005-097; RRID:AB_2337540
Biological samples		
Convalescent donor blood samples	The Kirby Institute, UNSW	https://kirby.unsw.edu.au/project/natural-history-cohort-following-sars-cov-2-infection
Donor blood samples	Australian Red Cross Lifeblood	https://www.donateblood.com.au/
Chemicals, peptides, and recombinant proteins		
RNase inhibitor	Takara Bio	Cat#2313A
dNTP	Promega Corporation	Cat#U1515
Triton X-10	Sigma-Aldrich	Cat#T9284
Polyfect Transfection Reagent	QIAGEN	Cat#301105
Glo Lysis Buffer	Promega	Cat#E2661
Polybrene	Sigma-Aldrich	Cat#H9268
TMB Chromogen Solution	ThermoFisher Scientific	Cat#002023
Imidazole	Sigma-Aldrich	Cat#I202
ExpiFectinamine	ThermoFisher Scientific	Cat#A14524
OptiMEM-1	ThermoFisher Scientific	Cat#31985070
Critical commercial assays		
Calphos transfection kit	Clontech Laboratories	Cat#631312
Bright-Glo Luciferase Assay System	Promega	Cat#E2620
Biotin Protein Ligase	Genecopeia	Cat#BI001
Experimental models: cell lines		
Expi293-Freestyle cells	ThermoFisher Scientific	Cat#A14527
CD81KO 293T	Dr Joe Grove	N/A
293T-ACE2 overexpressed calls	A/Prof Jesse Bloom	N/A
Lenti-X 293T	Clontech Laboratories	Cat#632180

(*Continued on next page*)

Continued

REAGENT or RESOURCE	SOURCE	IDENTIFIER
Oligonucleotides		
Primers for B cell receptor (BCR) amplification using SmartSeq2, see Table S1	N/A	N/A
Primers for backbone (C, H, κ and λ) fragment cloning PCR, see Table S1	N/A	N/A
Primers for varable (V_H, $V_κ$ and $V_λ$) fragment PCR, see Table S1	N/A	N/A
Primers for expression cassette assemble overlapping PCR, see Table S1	N/A	N/A
Recombinant DNA		
pCAGGS-SARS-CoV-2-RBD	This paper	N/A
pCAGGS-SARS-CoV-2-Spike	Dr Markus Hoffmann	N/A
pCAGGS-SARS-CoV-2-SpikeΔ18	Dr Markus Hoffmann	N/A
pTG126	Prof François-Loïc Cosset	N/A
phCMV5349	Prof François-Loïc Cosset	N/A
Software and algorithms		
GraphPad Prism	GraphPad	https://www.graphpad.com/scientific-software/prism/
FlowJo version 10.7.1	Tree Star, Inc	https://www.flowjo.com/
SPSS 25	IBM	https://www.ibm.com/products/spss-statistics
R 4.0.2	The R Foundation	https://cran.r-project.org/bin/windows/base/

RESOURCE AVAILABILITY

Lead contact

Further information and requests for resources and reagents should be directed to the lead contact, Dr. Rowena Bull (r.bull@unsw.edu.au)

Materials availability

This study did not generate new unique reagents.

Data and code availability

The published article includes all data generated or analyzed during this study, and summarized in the accompanying tables, figures and Supplemental information.

EXPERIMENTAL MODEL AND SUBJECT DETAILS

Human subjects

Convalescent COVID-19 donors

The COSIN (Collection of COVID-19 Outbreak Samples in NSW) study is an ongoing prospective cohort study evaluating the natural history of SARS-CoV-2 infection among adults and children in New South Wales, Australia. Children and adults diagnosed with SARS-CoV-2 infection (confirmed by NAT) were eligible for enrolment, irrespective of disease severity. Participants were enrolled through seven hospital in- and outpatient departments and referring microbiology laboratories in New South Wales between 6th March 2020 and 17th September 2020. Eighty-one participants were included in this study and had a median age of 51 years (IQR: 34 – 63.5 years) and 51% were female (n = 41) (Table 1).

Follow up visits were scheduled at one month (visit window: one to three months) and four months (visit window: four to six months) following symptom onset or date of diagnosis (whichever was first). At each follow up visit, clinical data and blood samples were collected. Disease severity was classified according to the NIH stratification (https://www.covid19treatmentguidelines.nih.gov).

Healthy unexposed donors

Healthy controls for antibody studies had a median age of 45 (range 24-73) and 53% were female. Blood from 10 of the healthy controls were collected prior to 2007 and the remaining 9 were collected between March and April 2020 in Sydney, Australia, where local

transmission was very low at the time. None of these 9 healthy controls had a history of COVID-19, were not close contacts of cases of COVID-19 and were not health care workers. For the memory B cell assays stored PBMCs from two of these healthy controls and stored PBMCs from four Australian Red Cross Lifeblood donors collected prior to 2020 were used (median age 38, range 25 to 48).

Ethics statement

The protocol was approved by the Human Research Ethics Committees of the Northern Sydney Local Health District and the University of New South Wales, NSW Australia (ETH00520) and was conducted according to the Declaration of Helsinki and International Conference on Harmonization Good Clinical Practice (ICH/GCP) guidelines and local regulatory requirements. Written informed consent was obtained from all participants before study procedures.

Cell lines

All 293T human embryonic kidney cells and Vero E6 cell were maintained at 37°C, 5% CO2 and > 90% relative humidity in growth medium containing high glucose Dulbecco's Modified Eagle Medium (ThermoFisher Scientific) supplemented with 10% v/v heat inactivated fetal bovine serum (Life Technologies; ThermoFisher Scientific). Expi293-Freestyle cells (ThermoFisher Scientific) were cultured at 37°C and 8% CO_2 in growth medium containing Expi293 Expression Medium (ThermoFisher Scientific).

Primary cells

Primary PBMCs were cryopreserved RPMI media supplemented with 2 mM L-glutamine, 50 IU/mL penicillin, 50 μg/mL streptomycin and 10% v/v DMSO. Prior performing experiments, cryopreserved PBMCs were thawed rapidly in a 37°C waterbath and washed with pre-warmed RPMI media supplemented with 2 mM L-glutamine, 50 IU/mL penicillin, 50 μg/mL streptomycin and 10% heat inactivated fetal calf serum (Sigma). The cells were resuspended in DPBS and stained for RBD specific memory B cells.

METHOD DETAILS

RBD and spike protein production

SARS-CoV-2 Spike RBD (residues 319-541), with a N-terminal human Ig kappa leader sequence and C-terminal Avi- and His-tags, was cloned into pCEP4 (Invitrogen). Expi293-Freestyle cells (ThermoFisher Scientific) were cultured at 37°C and 8% CO_2 in growth medium containing Expi293 Expression Medium (ThermoFisher Scientific). The plasmid was transiently transfected into Expi293-Freestyle cells as follows: $1.5x10^8$ total cells (50mL transfection) were mixed with 50 μg of plasmid, 160 μL of Expifectamin and 6 mL of OptiMEM-I and left overnight at 37°C in a shaking incubator. The following day 300 μL of ExpiFectamine Enhancer 1 and 3 mL of ExpiFectamine Enhancer 2 was added to the cells before the cells were left in culture for a further 48 hours. After a total of 72 hours in culture, the cell culture is collected and centrifuged for 20 minutes at 4000xg, 4°C. Cellular debris was clarified by passing the supernatant twice through a 0.22 μM filter. The His-tagged protein was then affinity purified from the cell supernatant using a HisTrap HP Column (GE Healthcare) and eluted with imidazole. The purified protein was then buffer exchanged and concentrated in sterile DPBS by centrifuging at 4000xg for 30 minutes at 4°C in a 10,000 MWCO Vivaspin centrifugal concentrator (Sartorius) and stored at – 80°C. The recombinant RBD was biotinylated using the Avitag as described by the manufacturer (Genecopeia).

RBD binding and limit of detection

Nunc-Immuno MicroWell plates, 96 well (ThermoFisher Scientific) were prepared with 250 ng of recombinant SARS-2 RBD protein in DPBS and incubated overnight at 4°C. The plates were washed with PBS containing 0.05% Tween-20 (PBS-T) and blocked with 5% non-fat milk for an hour at room temperature (RT). Heat inactivated (56°C for 30 minutes) patient serum or monoclonal antibodies were 3-fold serially diluted (1/20 to 1/1,180,980) in 5% non-fat milk, added to the plates in duplicate and incubated for two hours at RT. Anti-human IgG-HRP (Jackson Immunoresearch) was added at a 1:3000 dilution to the plates for one hour at room temperature. Binding of patient serum was detected using TMB Chromogen Solution (ThermoFisher Scientific) for 15 minutes at RT and the reaction was stopped using 1 M HCl. Optical density (OD) at 450 nm was measured using CLARIOstar microplate reader (BMG Labtech). The background level in SARS-2 RBD was determined by adding 2 SD to the mean OD_{450} of the highest dilution (1/20) of sera from 20 healthy unexposed individuals.

Anti-Spike antibody assay

A flow cytometry live cell-based assay was used to detect patient serum SARS-COV-2 Spike IgG antibodies as previously performed for neuroimmunological assays.[27] Spike (Wuhan strain) was expressed on transfected HEK293 cells. Serum was added to live spike-expressing cells, followed by staining with Alexa Fluor 647-conjugated anti-human IgG (H+L) (ThermoFisher Scientific). Cells were acquired on the LSRII flow cytometer (BD Biosciences). Participants were determined Spike antibody-seropositive if their delta median fluorescence intensity (ΔMFI = transfected cells MFI – untransfected cells MFI) was above the positive threshold (mean ΔMFI+4SD of 24 pre-pandemic controls) in at least two of three quality-controlled experiments. Data was analyzed using FlowJo 10.4.1 (TreeStar).

SARS-CoV-2 pseudovirus neutralisation assay

All cells were cultured at 37°C and 5% CO_2 in growth medium containing high glucose Dulbecco's Modified Eagle Medium (ThermoFisher Scientific) supplemented with 10% v/v heat inactivated fetal bovine serum (Life Technologies; ThermoFisher Scientific). Retroviral SARS-CoV-2 pseudovirus were generated by co-transfecting expression plasmids containing SARS-CoV-2 Spike which were kindly provided by Dr Markus Hoffmann,[28] and the MLV gag/pol and luciferase vectors which were kindly provided by Prof. Francois-Loic Cosset,[29,30] in CD81KO 293T cells, which were kindly provided by Dr Joe Grove,[31] using mammalian Calphos transfection kit (Takara Bio). Culture supernatants containing pseudovirus were harvested 48 hours post transfection and clarified of cellular debris by centrifugation at 500xg for 10 minutes. SARS-2pp were concentrated 10-fold using 100,000 MWCO Vivaspin centrifugal concentrators (Sartorius) by centrifugation at 2000xg and stored at –80°C.

For neutralisation assays, the infectivity of pseudovirus were diluted in media to 1000 – 5000-fold more infectious than negative background (based on pseudovirus lacking SARS-CoV-2 Spike). Diluted pseudovirus were incubated for one hour with heat inactivated (56°C for 30 minutes) patient serum or cell culture supernatant containing monoclonal antibodies, followed by the addition of polybrene at a final concentration of 4μg/mL (Sigma-Aldrich), prior to addition to 293T-ACE2 overexpressed calls, which were kindly provided by A/Prof Jesse Bloom.[32] 293T-ACE2 cells were seeded 24 hours earlier at 1.5 × 104 cells per well in 96-well white flat bottom plates (Sigma-Aldrich). Cells were spinoculated at 800xg for two hours and incubated for two hours at 37°C, prior to media change. After 72 hours, the cells were lysed with a lysis buffer (Promega) and Bright Glo reagent (Promega) was added at a 1:1 ratio. Luminescence (RLU) was measured using CLARIOstar microplate reader (BMG Labtech). Neutralisation assays were performed in triplicates and outliers were excluded using the modified z-score method.[33] Percentage neutralisation of pseudovirus was calculated as $(1 - RLU_{treatment}/RLU_{no\ treatment}) \times 100$. Serum neutralisation cut-off was determined using ID50 values obtained from 20 unexposed healthy participants (mean + 2 SD). The neutralisation cutoff for the mAb containing cell culture media was determined as the mean + 2 SD of the reading generated from screening neutralisation of the negative transfection control (no DNA). This was calculated to be 25.42% so any mAb with a neutralisation percentage greater than 40 at 1/10 dilution was classified as having neutralising activity. The 50% inhibitory concentration (ID50 for serum and IC_{50} for mAbs) titer was calculated using non-linear regression model (GraphPad Prism).

SARS-CoV-2 live virus neutralisation assay

Two-fold dilutions of patient plasma samples were mixed with an equal volume of virus solution (8×10^3 TCID50/ml) and incubated at 37°C for 1 hour. After the virus-plasma incubation, 40 μl virus/plasma mixture was added in duplicates to Vero E6 cells seeded in 384-well plates at 5×10^3 cells per well in a final volume of 40 μl. Plates were then incubated for 72 hours at 37°C, 5% CO_2 and > 90% relative humidity. Cell nuclei were stained with Hoechst-33342 dye (NucBlue, Invitrogen) and each well was imaged by a high-content fluorescence microscopy system (IN Cell Analyzer 2500HS, Cytiva Life Sciences, Parramatta, Australia). Cell number counts per well were obtained with the automated InCarta image analysis software (Cytiva). The percentage of virus neutralisation was calculated using the following formula: Neutralisation (%) = (D-(1-Q)) × 100/D, where "Q" represents a well's nuclei count divided by the average nuclei count of the untreated controls (i.e., cells and media only, defined as 100% neutralisation), and "D" = 1-Q for the average positive infection control (i.e., cells + virus, without plasma, defined as 0% neutralisation). An average neutralisation value > 50% was defined as having neutralising activity.

Staining RBD memory B cells

The tetramerization method was adapted from a previously published method used for hepatitis C virus tetramers.[34] In brief, biotinylated RBD was incubated with Streptavidin-PE (SA-PE; Molecular probes; ThermoFisher Scientific,) in a molar ratio of 4:1. The streptavidin dye was added stepwise in $1/10^{th}$ volume increments to the biotinylated protein, for a total of 10 times with a 10 minute incubation at 4°C, in a rotating bioreactor, protected from light.

Cryopreserved PBMCs were thawed rapidly in a 37°C waterbath and washed with pre-warmed RPMI media supplemented with 2 mM L-glutamine, 50 IU/mL penicillin, 50 μg/mL streptomycin and 10% heat inactivated fetal calf serum (Sigma). The cells were resuspended in DPBS and counted. All subsequent incubations were performed protected from light. A maximum of 1×10^7 cells were stained with Fixable Viability Stain 700 (FVS700) (BD Bioscience in a 1:1000 dilution) and incubated at 4°C for 20 minutes, to differentiate the live cells from dead. Cells were washed twice with FACS wash buffer (DPBS + 0.1% BSA), followed by incubation with 5 μL Human Fc block (BD) per 2×10^6 cells at room temperature for 10 minutes, to block non-specific antibody binding. SARS-CoV-2-specific B cells were identified by staining with 1 μg/mL of RBD tetramer at 4°C for 30 minutes. All consecutive steps were done either at 4°C or on ice and washed twice. The cocktail for staining contained 50 μL stain brilliant buffer and the titrated combination of antibodies: 5 μL each of CD21 BV421, IgD BV510, CD10 BV605, CD19 BV711 and CD20 APC-H7, 10 μL of IgG BV786, 2 μL each of CD27 PE-CF594 and CD38 PE-Cy7, 2.5 μL HLA-DR BB515 and 0.5 μL CD3 BB700. All the reagents were from BD Bioscience. The cells were incubated with the staining cocktail at 4°C for 30 minutes. They were washed and resuspended in FACS wash buffer. A BD FACSAria III sorter was used to phenotype and either bulk sort, or single cell sort, the samples. The data analysis was performed using FlowJo version 10.7.1 (TreeStar).

Production of monoclonal antibodies from single-sorted RBD-specific B cells

Natively paired heavy and light chain variable (V_H and V_L) region sequences were obtained by amplifying the regions separately from single sorted B cells as previously described.[34] In brief, single sorted RBD-specific B cells ($CD19^+CD20^+CD10^-RBD^+$) were collected

into 96-well PCR plates that contained in a final volume of 2 μL per well: 0.5 μL of dNTP (10 mM) (ThermoFisher Scientific), 0.5 μl of 5 μM oligo-dT primer and 1 μL of lysis buffer, lysis buffer was prepared by addition of 1 μL (40 U) RNase inhibitor (Clontech) to 19 μL Triton X-10 (0.2% [v/v]). These samples were then RT-PCR amplified with the SmartSeq2 approach.[35]

Amplicons of the B cell receptor (BCR)-encoding regions were generated from the SmartSeq2 libraries, as described previously.[34,36] Amplicons were Sanger sequenced and analyzed with Immcantation.[37] Antibodies were generated by co-transfecting Lenti-X 293T cells (Clontech) with 1 μg each of heavy and light chain expression cassette using 20 μL of Polyfect Transfection Reagent (QIAGEN) and 600 μL of DMEM supplemented with 2 mM L-glutamine, and 10% heat inactivated fetal calf serum (Sigma). Cells were incubated at 37°C and 5% CO_2 for 6-8 hours before media was replaced with 3 mL of DMEM supplemented with 2% heat inactivated fetal calf serum and 1% penicillin/streptomycin, and incubated under the same conditions for a further 67-72 hours. Media was then collected and centrifuged to isolate supernatant containing antibodies, before storage at −20°C.

A RBD binding ELISA was performed on the undiluted mAbs, as described above for serum, to determine the specificity of the RBD tetramer-sorted memory B cells. Successful transfection and mAb synthesis was confirmed with a total IgG ELISA. In brief, Nunc-Immuno MicroWell plates, 96 well (Thermo Scientific,) were prepared with 1 μg of anti-human IgG (Jackson Immunoresearch) in DPBS and incubated for one hour at 37°C. The plates were washed with TBS containing 0.05% Tween-20 (TBS-T) and blocked with 5% non-fat milk for an hour at RT. The mAbs were added to the plates in duplicates and incubated for one hour at RT. Anti-human IgG-HRP (Jackson Immunoresearch) was added at a 1:6000 dilution to the plates for one hour at RT. Binding of mAbs was detected using TMB Chromogen Solution (ThermoFisher Scientific) for 15 minutes at room temperature and the reaction was stopped using 1 M HCl. Optical density (OD) at 450 nm was measured using CLARIOstar microplate reader (BMG Labtech).

QUANTIFICATION AND STATISTICAL ANALYSIS

The EPT and ID50 analyses were performed in GraphPad Prism 8.4.3. Wilcoxon or Mann-Whitney tests were applied for paired and unpaired analyses, respectively, to evaluate statistically significant differences between t1 and t2. EPT and ID50 values were fitted to a Loess curve using ggplot2 package in R 4.0.2 using stat_smooth() function with default parameters. Correlation analyses were performed using the non-parametric Spearman's test. ID50 and Spike binding data were plotted using a linear scale. EPT data were plotted using a log transformed scale. Statistical significance was set at $p < 0.05$.

Descriptive statistics are given as count data (for discrete variables) or as measures of central tendency and dispersion (for continuous data). ID50 and EPT were measured at two time points per subject (t1: 1-3 months post infection, t2: 4-6 months post infection) and their distributions were compared with a paired sample t test. Associations for variation of ID50 and EPT (dependent variables) were explored with a mixed model analysis for within (time) and between host effects, while considering time gap between sampling points as a covariate (using repeated-measures ANOVA). In the unadjusted analysis, each of the following independent (between-host) variables were compared: gender (male versus female), disease severity (asymptomatic or mild versus moderate or severe), immunosuppression, age, current or past history of smoking, metabolic comorbidities (either diabetes, hypertension or obesity). If any significant associations were noted, they were combined in an adjusted analysis (repeated-measures ANOVA). Statistical significance was set at $p < 0.05$.

In addition, associations were also explored for the fold decline of EPT and ID50 (dependent variable) across the two time points (e.g., ID50t2/ID50t1) with the same independent variables as above, using univariate analysis of variance. To remove extreme values of fold-change, the outlier participants were removed by only considering those within the interquartile range (Q1-Q3) for EPT and ID50 data arrays at the first time point.

For the memory B cell evaluation, statistical analysis was performed on log transferred data values. The number of CD27+ IgG+ RBD+ cells/10^6 B cells were measured at the two time points and their distributions was compared with a Wilcoxon matched-pairs signed rank test. A simple linear regression model was used to analyze the relationship between the memory B cell numbers and the age, ID50 and EPT at individual time points of each participant. A Mann Whitney test was performed to compare the inter/intra-gender and disease severity association with the RBD MBC numbers. A non-parametric Spearman's test was performed for correlation analysis.